

Spin Density and Non-Collinear Magnetization in Frustrated Pyrochlore $Tb_2Tl_2O_7$ from Polarized Neutron Scattering.

Arsen Gukasov¹, Huibo Cao¹, Isabelle Mirebeau¹ and Pierre Bonville²

¹Laboratoire Leon Brillouin, CEA-CNRS, CE-Saclay, 91191 Gif-sur-Yvette, France.

²Service de Physique de l'Etat Condensé, CEA-CNRS, CE-Saclay, 91191 Gif-sur-Yvette, France.

Abstract

We used a local susceptibility approach in extensive polarized neutron diffraction studies of the spin liquid $Tb_2Tl_2O_7$. For a magnetic field applied along the [110] and [111] directions, we found that, at high temperature, all Tb moments are collinear and parallel to the field. With decreasing temperature, the Tb moments reorient from the field direction to their local anisotropy axes. For the [110] field direction, the field induced magnetic structure at 10 K is spin ice-like, but with two types of Tb moments of very different magnitudes. For a field along [111], the magnetic structure resembles the so-called "one in-three out" found in spin ices, with the difference that all Tb moments have an additional component along the [111] direction due to the magnetic field. The temperature evolution of the local susceptibilities clearly demonstrates a progressive change from Heisenberg to Ising behavior of the Tb moments when lowering the temperature, which appears to be a crystal field effect.

Key words: Polarized neutron, frustrated magnets, pyrochlore
 PACS: 71.27.+a, 75.25.+z, 61.05.fg

1. Introduction

Recent polarized neutron studies of the magnetic distribution in some ferromagnetic and paramagnetic materials with the Tl_3P_4 cubic structure have shown that the moment induced by a magnetic field at equivalent crystallographic sites may be very different [1,2,3]. Such a behavior can arise when the local symmetry of the magnetic ion is lower than the overall symmetry of the crystal. The moment induced on each magnetic ion by the internal or external magnetic field depends on the orientation of the field with respect to the local symmetry axis. This effect can be described by attributing to each magnetic atom a site susceptibility tensor χ_{ij} which gives the magnetic (linear) response of the ion to the applied magnetic field H_i . The symmetry of the χ_{ij} tensor is the same as that of the u_{ij} tensor describing the thermal motion of atoms. The components of the u_{ij} tensor represent the mean square atomic displacement parameters (ADPs). In the linear approximation, i.e. for relatively weak magnetic fields, one can introduce atomic susceptibility parameters (ASPs) in a way analogous to the ADPs. The response of an atom to a magnetic field can then be conveniently visualized as a magnetization ellipsoid constructed from the six independent

ASPs in much the same way as thermal ellipsoids are constructed from the ADPs. In the absence of local anisotropy the magnetic ellipsoids reduce to spheres with their radii proportional to the induced magnetization, but in many cases anomalous (elongated or flattened) ellipsoids can appear. The presence of such anisotropic magnetic ellipsoids accounts for the anomalous magnetic behavior mentioned above.

$R_2Tl_2O_7$ pyrochlore compounds represent another type of a cubic structure with space group $Fd\bar{3}m$ where the local symmetry of the magnetic ion is lower than the overall symmetry of the crystal. In $R_2Tl_2O_7$, the rare earth ions occupy a 16d site with a local trigonal symmetry $3m$ and are subject to a strong crystal field interaction. Both the R and Tl atoms independently lie on a pyrochlore structure, a face-centered cubic lattice of corner sharing tetrahedra which produces phenomena of geometrical frustration. Depending on the nature of the magnetic rare earth ion in these materials, the ground state can exhibit long range magnetic order [5,6] or spin ice physics [7,8], and in the case of $Tb_2Tl_2O_7$ it is a highly correlated quantum disordered state known as a spin liquid [9,10,11]. In $Tb_2Tl_2O_7$ [12,13] the anisotropy is weaker than in canonical spin ices, and ferromagnetic (F) and antiferromagnetic (AF) first neighbor interactions

nearly compensate. This makes $Tb_2T_{1/2}O_7$ extremely sensitive to external perturbations, which leads to a rich variety of magnetic ground states, from spin liquid [9] to antiferromagnetic order under pressure [14] and/or in magnetic field [15,16]. We undertook a systematic study of the field induced magnetic orders in the spin liquid $Tb_2T_{1/2}O_7$ in a wide temperature ($0.3 < T < 270$ K) and field ($0 < H < 7$ T) range, by combining polarized and unpolarized neutron diffraction on a single crystal. Unpolarized neutron results will be published elsewhere [17,18]; we describe here in detail our polarized neutron results based on the local susceptibility approach. We show that this approach is extremely efficient in the treatment of polarized neutron data as it allows an universal description of magnetic structures existing in large temperature (5–300 K) and field (1–7 T) ranges, regardless of the field direction, with only 2 parameters.

2. Experimental

Neutron diffraction studies were performed on the diffractometer Super-6T2 [19] and 5C1 at the ORPHEE reactor of the Leon Brillouin Laboratory, CEA/CNRS Saclay. Polarized neutron flipping ratios were measured on Super-6T2 using neutrons with $\lambda = 1.4$ Å obtained with a supermirror bender ($P_0 = 0.98$) and completed by measurements on 5C1 ($\lambda = 0.84$ Å) obtained with a Heussler polarizer ($P_0 = 0.91$). The programs CHLSQ of the Cambridge Crystallography Subroutine Library [20] and MEND [21] were used for the least squares refinements on the flipping ratios and maximum entropy reconstruction respectively.

A single crystal of $Tb_2T_{1/2}O_7$ was grown from a sintered rod of the same nominal composition by the coating-zone technique, using a mirror furnace [17]. Prior to polarized neutron measurements the crystal was characterized by neutron diffraction at 180 K and 2 K in zero-field. A total of 238 reflections with $\sin \theta < 0.6$ Å⁻¹ was measured at 2 K. The structure factors of 46 unique reflections were obtained by averaging equivalents. These were used to refine all positional parameters, the occupancy factors, the isotropic temperature factors and the extinction parameters. The refinement of the crystal structure was performed using space group $Fd\bar{3}m$.

3. Magnetic ellipsoids and anisotropic susceptibility parameters

According to Ref. [4] atomic (local) susceptibility parameters can be determined from polarized neutron flipping ratio measurements if the proper magnetic symmetry of the crystal is taken into account. In order to investigate the temperature dependence of local susceptibilities of $Tb_2T_{1/2}O_7$, a series of flipping ratio measurements was made at 1.6, 5, 10, 20, 50, 100, 150, 200 and 270 K with a magnetic field of 1 T applied parallel to the [110] direction. (In fact there was a misalignment of about 5 degrees be-

tween the [110] direction and the magnetic field direction. The exact orientation of the magnetic field with respect to the cubic crystal axes was taken properly into account in the final data analysis.) The results were interpreted in terms of a model which assigns a site susceptibility tensor to each crystallographically independent site [4]. The point group symmetries of the atomic sites of the paramagnetic group $Fd\bar{3}m$ were used to constrain the site susceptibility tensors. In the cubic axes, the symmetry constraints for a magnetic atom occupying the 16d site in the $Fd\bar{3}m$ group imply: $\chi_{11} = \chi_{22} = \chi_{33}$ and $\chi_{12} = \chi_{13} = \chi_{23}$. Thus, only two independent susceptibility parameters χ_{11} and χ_{12} need to be determined regardless of the field direction.

For each temperature these two independent components χ_{11} and χ_{12} were determined using the least squares refinement program CHLSQ [20]. The refinement carried out with the 102 flipping ratios measured at 270 K with the magnetic field $H = 1$ T applied parallel to [110] gave $\chi_{11} = 0.056(5)$ χ_B/T and $\chi_{12} = 0.005(6)$ $(11) \chi_B/T$ with a goodness of $\chi^2 = 1.02$. For convenience, the susceptibility components are given in χ_B/T , which allows an easy comparison with the results of a conventional least squares refinement based on the localized magnetic moment model. The fact that the non-diagonal term χ_{12} is equal to zero (within error bars) shows that the magnetic ellipsoids at 270 K reduce to spheres of diameter $0.056 \chi_B/T$. It means that the moments induced on all Tb atoms in the unit cell have the same magnitude and are collinear with the magnetic field regardless of the field direction. This behavior resembles that of a Heisenberg paramagnet at high temperature. The situation is quite different at low temperature where the refinement carried out with the 423 flipping ratios measured at 10 K in the same magnetic field gave $\chi_{11} = 0.939(15)$ χ_B/T and $\chi_{12} = 0.535(11) \chi_B/T$ with the goodness of $\chi^2 = 2.92$. One can see that, besides a considerable increase of the diagonal term χ_{11} reflecting the Curie-Weiss behavior, the non-diagonal elements χ_{12} become very large, showing that the principal axes of the magnetic ellipsoid are different in length and do not coincide with the cubic crystal axes. It is easy to show that the trigonal local symmetry implies that the main principal axes of the ellipsoids lie along the four [111] axes and their lengths are given by: $\chi_k = \chi_{11} + 2\chi_{12}$ and $\chi_\perp = \chi_{11} - \chi_{12}$.

The evolution of the magnetic ellipsoids with temperature is illustrated in Fig. 1. One can see that the shape and the mutual orientation of the ellipsoids reflect the cubic symmetry of the structure. The ratio of the length of the main axes, χ_k along the local anisotropy (trigonal) axis [111] and χ_\perp perpendicular to it, is strongly temperature dependent and the ellipsoid elongation, which is due to an enhancement of the χ_{12} component, increases markedly at low temperatures. Magnetization along the easy and hard local axes at 10 K differ by a factor of 5, which shows that the local anisotropy progressively evolves from Heisenberg to Ising character when the temperature decreases.

Once the site susceptibility parameters are known, one can easily calculate the magnitude and the direction of the

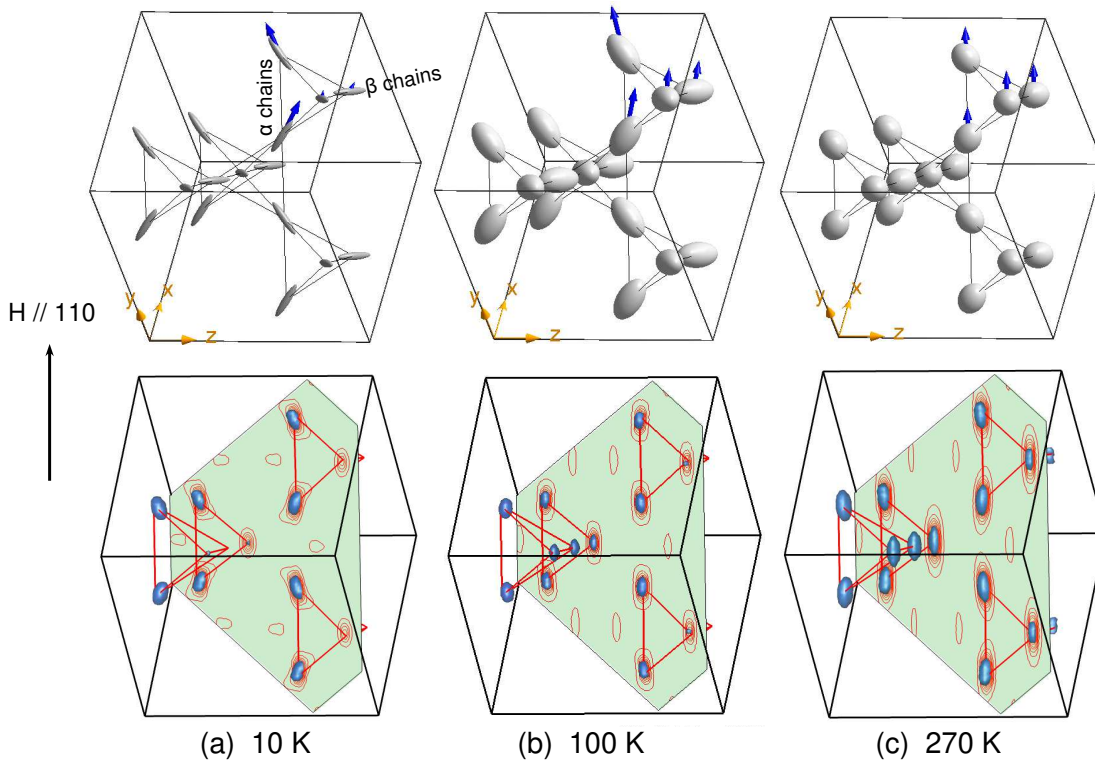


Fig. 1. Top: Magnetic structure (arrows) and magnetic ellipsoids measured in the field $H = 1$ T k to [110] at 10 K (a), 100 K (b) and 270 K (c). Ellipsoids were scaled by temperature to compensate the Curie-Weiss behavior. Bottom: Two dimensional (2D) sections of the magnetization density component m_z parallel to the field (red contours) and three dimensional (3D) isosurfaces of the magnetization density m_z (blue). The level of the isosurface selected on each figure corresponds to 25% of the maximum density in the cell found in the reconstruction. The maximum values of densities are scaled by temperature.

moment induced on each Tb atom by a magnetic field applied in an arbitrary direction since the site susceptibility tensor relates the vectors M on each Tb ion and $H : M = H$. The magnetic structures at 10, 100 and 270 K resulting from the refinement are shown in Fig. 1. There is a progressive evolution of the structure from collinear, with the same magnetic moment on all Tb ions, to non-collinear with two types of Tb ions having a high and a low moment. This corresponds to the separation of Tb ions into so-called α and β -chains [23,24]. Moments in β -chains have their local $\langle 111 \rangle$ easy axis close to H (35.3°), whereas moments in α -chains have their easy axis perpendicular to H . The non-collinear magnetic structure induced at low temperature by the field can be seen as a direct consequence of the strong local anisotropy, the moments remaining close to the elongated axes of the ellipsoids whatever the field direction.

To verify the validity of the local susceptibility approach, a second series of flipping ratio measurements was performed with a field of 1 T parallel to the [111] direction at different temperatures. Refinement on 144 flipping ratios at 10 K gave $r_{11} = 0.95(5)$ B and $r_{12} = 0.55(4)$ B with $\chi^2 = 7.1$. The r_{ij} parameters for the [111] field direction coincide within experimental error with those obtained for the field along [110]. The magnetic structure at 10 K resulting from the refinement is shown in Fig. 2. One can easily recognize the so-called "one in-three out" spin con-

figuration described earlier in Ref. [23], with the difference that all Tb moments have additional components along the [111] direction due to the magnetic field. These results confirm that the polarized neutron data collected with different field orientations can be interpreted within the paramagnetic group $Fd\bar{3}m$ using only the 2 susceptibility parameters allowed by symmetry.

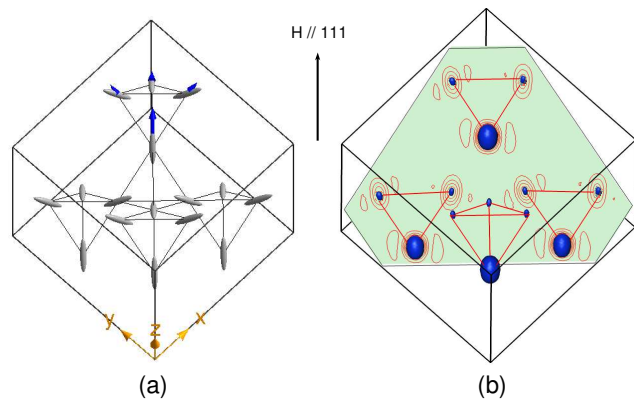


Fig. 2. a) Magnetic structure and magnetic ellipsoids measured in a field $H = 1$ T k to [111] at 10 K. b) The corresponding 2D map and 3D isosurface of the magnetization density m_z , see captions to Fig. 1.

4. Magnetization densities

Our refinements show a significant difference between the magnetic moments in a - and c -chains and it is useful to check to what extent this result can be substantiated by a model-free analysis of our data by the maximum entropy method (MEM). This method has been shown to give much more reliable results than conventional Fourier syntheses, by considerably reducing both noise and truncation effects [22]. In order to carry out the MEM reconstructions the magnetic structure factors of all data sets were extracted from flipping ratios using the SORGAM program [20].

As shown in Ref. [2] when the local symmetry of the magnetic ion is lower than the overall symmetry of the crystal, the high symmetry paramagnetic group $Fd\bar{3}m$ cannot be used in the magnetization density reconstruction. For the field oriented along the two-fold axis [110], for example, the low symmetry (orthorhombic) $Fdd2$ group must be used. This is the highest symmetry subgroup of $Fd\bar{3}m$ under which the homogeneous magnetization component m_z , induced parallel to the two-fold axis by the magnetic field, is invariant. An important consequence of the symmetry reductions is that the number of independent reflections to be measured increases considerably compared to that of the paramagnetic group. A typical number of reflections used in the reconstruction varies from 100 to 400, depending on the degree of local anisotropy and on the magnitude of the flipping ratios. The magnetization density distribution was discretized into $51 \times 51 \times 51$ sections along a , b and c respectively. Then the magnetization density component parallel to the field (m_z) was reconstructed using a conventional uniform (at) density [22]. Results of the reconstruction are presented in Fig. 1 a-c. For each temperature, the figure shows both a 2D section of the magnetization density in the [111] plane and a 3D isosurface of the density. One can see that at 270 K the magnetization isosurface is nearly the same on a - and c -chains, while at 10 K magnetization is practically absent on the c -chains. Thus the reconstruction confirms the presence of a large difference of m_z components of the Tb moment in a - and c -chains at low temperature, in spite of the fact that the maximum entropy method is strongly biased against a disequilibrium of magnetic density in the unit cell. We note also that sections through a Tb site at 10 K show that the magnetization density on c -chains is elongated in the [111] directions (Fig. 1 a, bottom). This might be a consequence of the strong crystal field anisotropy at low temperature. We stress that, in the above figures, we only present the m_z component of the density as the flipping ratio measurements can only yield the density component collinear with the field. On the other hand the presence of a high degree of anisotropy in the local susceptibility implies a considerable non-collinearity on the magnetization distribution at low temperature. To account for this, more sophisticated neutron experiments are needed [25]. We suggest that the non-collinear part of the magnetization density can proba-

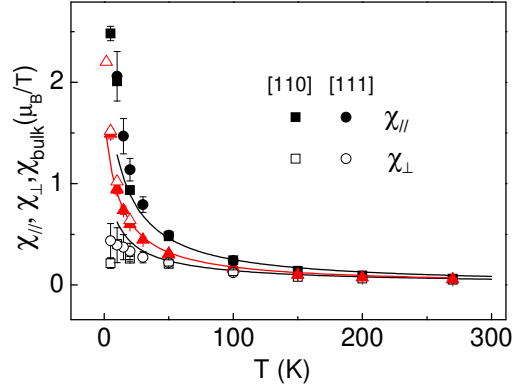


Fig. 3. Longitudinal and transverse local susceptibilities $\chi_{||}$ and χ_{\perp} versus T . Square and circle symbols correspond to a field along [110] and [111] respectively. Filled triangles show the bulk susceptibility derived from the neutron data, $\chi_{\text{bulk}} = 1/3 \chi_{||} + 2/3 \chi_{\perp}$, open triangles the bulk susceptibility from Ref. [13]. Lines are calculations using the CF parameters of $Tb_2T_{12}O_7$ (see text).

ably be extracted by combining flipping ratio and integrated intensity measurement in a magnetic field, but this needs to be verified experimentally.

A similar maximum entropy reconstruction (using a trigonal symmetry subgroup of $Fd\bar{3}m$) was performed on flipping ratios measured with the field parallel to [111]. The resulting magnetization density component m_z obtained at 10 K in 1 Tesla is shown in Fig. 2. It gives an evidence that Tb ions having their local axis parallel to the field have a very high magnetic moment, while the rest of the Tb ions have very small moments, in agreement with the biased "one in-three out" structure obtained by the refinement (bottom Fig. 1 a).

5. Longitudinal and transverse local susceptibilities

Figure 3 shows that the ratio of the main axes of the ellipsoids $\chi_{||}/\chi_{\perp}$ increases with decreasing temperature. This reflects the increasing CF anisotropy as temperature decreases. Indeed, at high temperature, many CF states are populated and the anisotropy is close to that of the free ion (weak or Heisenberg-like), whereas at low temperature, the lowest doublets alone are populated, which have a strong Ising behaviour. The local susceptibilities obtained with the field along [110] and [111] are in a very good agreement, which confirms that this approach is valid regardless the field orientation.

For comparison with the experimental data, we used the CF parameters of $Tb_2T_{12}O_7$ derived from the inelastic neutron spectra [13]. The parameters account properly for the trigonal symmetry of the Tb environment and allow to compute magnetization induced by a magnetic field applied parallel or perpendicular to the local $\langle 111 \rangle$ axis. Interatomic exchange and dipolar interactions were taken into account in the molecular field approximation via a microscopic constant J . The self-consistent calculation, valid

down to 10 K, yields a constant $\chi = -0.35 \text{ T} / B$, close to the value derived in Ref. [13]. The result of the calculations agrees well with the experiment, see Fig. 3.

In the local susceptibility approach, the atomic site susceptibility tensor accounts only for the linear paramagnetic response of the moments to an applied field. The range of fields and temperatures satisfying the condition of linear response can be estimated from the bulk magnetization data [13]: the χ_{ij} parameters obtained in our refinement allow the general behavior of $\text{Tb}_2\text{T}_{1/2}\text{O}_7$ to be described above 10 K in fields up to 7 T applied in an arbitrary direction.

6. Conclusion

We determined the field induced magnetic structures in $\text{Tb}_2\text{T}_{1/2}\text{O}_7$ by polarized neutron diffraction, in a wide range of temperatures and fields, applied in the [110] or [111] directions. The [110] low temperature ground state shows a non-collinear magnetic structure that resembles the local spin ice ground configuration, but with Tb moments of very different magnitudes. The [111] low temperature ground state is close to the structure "one in-three out" found in spin ices, with the difference that all Tb moments have an additional component along the [111] direction due to the magnetic field. This is attributed to the finite CF anisotropy of $\text{Tb}_2\text{T}_{1/2}\text{O}_7$ which is much weaker than in model spin ices. Polarized neutron diffraction and the local susceptibility approach provide an easy way for studying field induced structures in pyrochlore compounds. They provide a universal description of the magnetic structures in $\text{Tb}_2\text{T}_{1/2}\text{O}_7$ in a large range of fields and temperatures, with only two local susceptibility parameters regardless of the field direction.

We thank P. J. Brown for help in using CCSL and interesting discussions and G. Dhalenne for the crystal synthesis. H. Cao acknowledges support from the Triangle de la Physique.

References

- [1] A. Gukasov, P. Wisniewski and Z. Henk. *J. Phys. Condens. Matter*, **8**, 10589, 1996
- [2] Boucherle J-X, Givord F, Schweizer J, Gukasov A, Mignot J-M, Lelievre-Berna E, Aoki H and Ochiai A. *Physica B* 267-268, 37-40, 1999
- [3] Boucherle J-X, Givord F, Schweizer J, Gukasov A, Mignot J-M, Lelievre-Berna E, Aoki H and Ochiai A. *Physica B*, 281-282, 139-140, 2000
- [4] A. Gukasov and P. J. Brown. *J. Phys. Condens. Matter*, **14**, 8831, (2002)
- [5] J. D. M. Champion, M. J. Harris, P. C. W. Holdsworth, A. S. Wills, G. Balakrishnan, S. T. Bramwell, E. Cizmari, T. Fennell, J. S. Gardner, J. Lago, D. F. McMorrow, M. Orendac, A. Orendacova, D. McKPaul, R. I. Smith, M. T. F. Telling, and A. Wildes. *Phys. Rev. B* **68**, 020401(R) (2003).
- [6] N. P. Raju, M. Dion, M. J. P. Gingras, T. E. Mason, and J. E. Reedan. *Phys. Rev. B* **59**, 14489 - 14498, (1999).
- [7] M. J. Harris, S. T. Bramwell, D. F. McMorrow, T. Zeiske and K. W. Godfrey. *Phys. Rev. Lett.* **79**, 2554-2557, (1997).
- [8] B. C. den Hertog, and M. J. P. Gingras, *Phys. Rev. Lett.* **84**, 3430 (2000).
- [9] Gardner J S et al *Phys. Rev. Lett.* **82** 1012 (1999).
- [10] J. S. Gardner, B. D. Gaulin, A. J. Berlinsky and P. Waldron, S. R. Dunsiger, N. P. Raju, and J. E. Reedan, *Phys. Rev. B* **64**, 224416 (2001).
- [11] J. S. Gardner, A. Keren, G. Ehlers, C. Stock, E. Segal, J. M. Roper, B. Fak, M. B. Stone, P. R. Hammar, D. H. Reich and B. D. Gaulin. *Phys. Rev. B* **68**, 180401 R1-4, (2003)
- [12] Gingras M J P et al 2000 *Phys. Rev. B* **62** 6496
- [13] I. Mirebeau, P. Bonville, and M. Hennion, *Phys. Rev. B* **76**, 184436 (2007).
- [14] I. Mirebeau, I. N. Goncharenko, P. Cadavez-Peres, S. T. Bramwell, M. J. P. Gingras, and J. S. Gardner, *Nature* **420**, 54 (2002).
- [15] I. Mirebeau, I. N. Goncharenko, G. Dhalenne and A. Revcolevschi, *Phys. Rev. Lett.* **93**, 187204 (2004).
- [16] K. C. Rule, J. P. C. Ruff, B. D. Gaulin, S. R. Dunsiger, J. S. Gardner, J. P. C. Lancy, M. J. Lewis, H. A. Dabkowska, I. Mirebeau, P. Manuel, Y. Qi, and J. R. D. Copley, *Phys. Rev. Lett.* **96**, 177201 (2006)
- [17] Cao H, Gukasov A, Mirebeau I, Bonville P and Dhalenne G 2008 (unpublished).
- [18] Cao H, Gukasov A and Mirebeau I 2008 (unpublished)
- [19] A. Gukasov, A. Goujon, J.-L. Mercurio, C. Person, G. Exil, and G. Koskas, *Physica B* **397**, 131134 (2007).
- [20] P. J. Brown et al., CCSL, RAL 93-009, 1993.
- [21] M. Sakata, R. Mori, S. Kumazawa, M. Takata and H. Toraya *J Appl Cryst.* **23**, 526-534, (1990)
- [22] R. J. Papoulik and B. Gillon. *Europhys. Lett.*, **13**, 429 (1990)
- [23] Hiroi Z, Matsuhira K and Ogata M 2003 *J. Phys. Soc. Jpn.* **72** 3045
- [24] Ru J P C, Melko R G and Gingras M J P 2005 *Phys. Rev. Lett.* **95** 097202
- [25] P. J. Brown. *J. of Phys. Chem. Solids*, **65**, 1977, 2004